Rit Veðurstofu Íslands

Sigurður Th. Rögnvaldsson
Gunnar B. Guðmundsson
Kristján Ágústsson
Steinunn S. Jakobsdóttir
Ragnar Slunga
Ragnar Stefánsson

Overview of the 1993-1996 seismicity near Hengill

VÍ-R98006-JA05
Reykjavík
September 1998

ISSN 1025-0565
ISBN 9979-878-13-4

Sigurður Th. Rögnvaldsson
Gunnar B. Guðmundsson
Kristján Ágústsson
Steinunn S. Jakobsdóttir
Ragnar Slunga
Ragnar Stefánsson

Overview of the 1993-1996 seismicity near Hengill

VÍ-R98006-JA05
Reykjavík
September 1998

CONTENTS

1 SUMMARY

From July 1994 through most of 1996 seismic activity was unusually high in the rift zone near the Hengill triple junction in SW-Iceland. The largest events reached magnitude 4.2. Faulting was mostly strike-slip on near-vertical planes. The average direction of maximum horizontal compression released in these earthquakes was 53°E. This mode of faulting is similar to that observed in the transform zone in southern Iceland but different from the type of faulting associated with the last major rifting episode at this part of the divergent plate boundary in 1789. Accurate relative locations were determined for 1680 earthquakes, utilizing the cross-correlation of their waveforms. The relocated earthquakes often form dense groups that delineate planar surfaces. We interpret the planes defined by such groups as common fault planes for events in each group. From the relative locations we have determined the strike and dip of 28 active faults. Faults near the transform zone have northerly strikes, in agreement with field observations. Within the Hengill volcanic system the fault strikes are more varied, with N-S, E-W and N25°E being the most common directions. We suggest that this variability reflects reactivation of existing faults that initially ruptured in a stress field with an orientation different from today's field. The total moment released in the episode from 1993 to 1996 corresponded roughly to a single M = 5 event.

2 INTRODUCTION

The Hengill area in SW-Iceland is located at the junction of the western rift zone (WRZ in Figure 1), the South Iceland seismic zone (SISZ) and the on-land continuation of the Reykjanes ridge (RR), the Reykjanes peninsula. The WRZ is a 10–15 km wide zone of rifting and recent volcanism trending NNE. The SISZ is an east trending transform zone which accommodates the rift in the eastern rift zone (ERZ) and on the Reykjanes ridge. The trend of the plate boundaries west of the junction, as defined by seismicity, is WSW.

The Hengill area is a complex of volcanos and fissure swarms (Árnason et al. 1985). In Figure 1 Hv is the extinct and deeply eroded Hveragerði central volcano. The most pronounced geological and tectonic feature in the area is the Hengill volcano system (He in Figure 1), which is about 7 km NW of the Hveragerði central volcano. Its graben-like fissure swarm is 80 km long and 4–5 km wide and defines the west border of the WRZ in the region. Hrómundartindur volcano (Hr in Figure 1) is located between the Hengill and Hveragerði volcanic centers. The largest part of the bedrock consists of hyaloclastites from the last ice-age but several post-glacial fissure eruptions have taken place in the area, the last one 2000 years ago.

Magnetic, topographic and resistivity anomalies are observed trending WNW from Mt. Hengill, i.e. orthogonal to the WRZ. Fissures with this trend are observed farther west in Mt. Hengill and hot springs and earthquake swarms align it. Hydrothermal activity is widespread in the area and extensive geophysical investigations have been carried out in connection with the utilization of the geothermal energy. The results are summarized in several reports and articles, e.g. Sæmundsson (1967); Hersir et al. (1990); Árnason (1993); Foulger (1988a); Toomey and Foulger (1989) and references therein.

Geodetic measurements, including levelling of lines and GPS measurements show about 5 cm uplift near Mt. Hrómundartindur. These results have been interpreted as indicating an intrusion into the roots of Hrómundartindur volcano, causing both the uplift and recent seismicity (Sig-

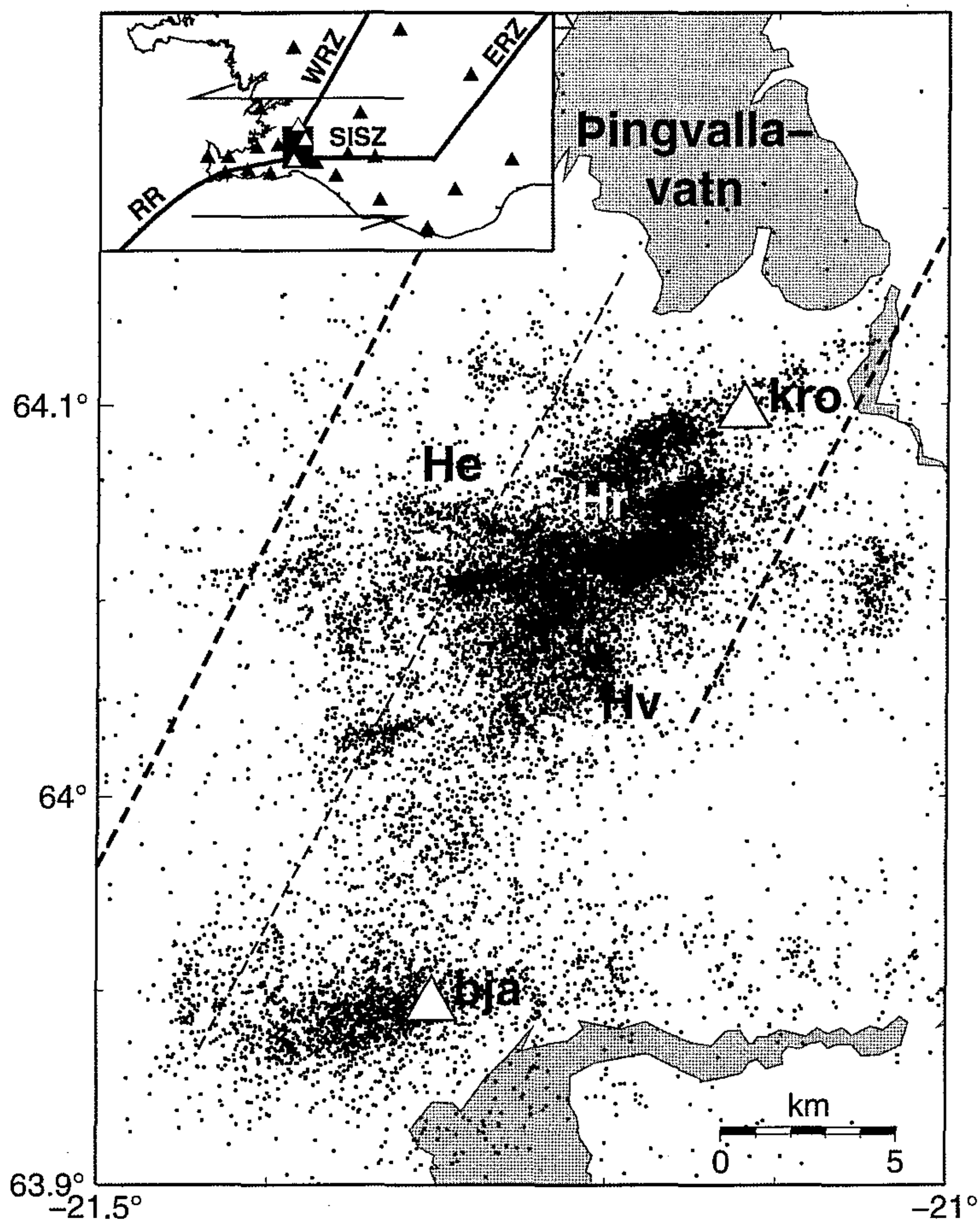

Figure 1. *The Hengill area in SW-Iceland. Rivers and lakes are shaded, dots denote earthquake epicenters during 1993–1996. Only events with* $M_w \geq 0.5$ *are shown. The inset figure shows the main tectonic features in SW-Iceland, the location of the Hengill area is marked with a black square. Arrows indicate the plate motion. WRZ and ERZ are the western and eastern rift zones, RR is the Reykjanes ridge and SISZ the South Iceland seismic zone. He, Hr and Hv are the Hengill, Hrómundartindur and Hveragerði volcanos. Seismic stations of the SIL network are denoted by triangles. The thick dashed lines indicate borders of the rift zone. The thin dashed line represents the eastern border of the Hengill fissure swarm.*

mundsson et al. 1997).

During the past 10000 years the average subsidence rate on the Hengill fissure swarm is about 4 m every 1000 years (4 mm/yr). The subsidence seems to happen both continuously and episodically (Árnason et al. 1985; Tryggvason 1990). The last major tectonic episode in the Hengill area, with both seismic activity and considerable ground deformation, occurred in 1789 (Halldórsson and Stefánsson 1986). Over 60 cm subsidence was observed at the northern shore of lake Þingvallavatn and up to 2 m on individual faults north of Mt. Hengill. Simultaneously uplift was observed along the flanks of the swarm (Halldórsson 1996). Continuous seismic activity lasted 10 days and individual earthquakes were felt for several months. The total strain release during the episode is estimated to be comparable to an earthquake of magnitude 6.5 (Halldórsson and Stefánsson 1986).

From 1952 to 1955 several earthquake swarms occurred in the Hengill area. The activity culminated in a magnitude 5.5 earthquake in 1955. Since then the activity in the area has remained relatively low until the onset of the present earthquake sequence in 1994. The location of the 1952–55 earthquakes is based mostly on one instrument in Reykjavík for the smaller events but larger events were detected at Akureyri in northern Iceland and at Kirkjubæjarklaustur in SE-Iceland. The location accuracy is of the order of ± 10 km. By taking into account information on felt earthquakes it can be concluded that the earthquakes covered all the area active in the present episode.

In this report we present the first results of analyzing earthquake data from the 1994–1996 seismic episode in the Hengill area, recorded by a regional network. The report is an extension of previous work, published in conference proceedings (Rögnvaldsson et al. 1996). The 1997 seismicity has been reviewed in an earlier report (Rögnvaldsson et al. 1998). Fault plane solutions of thousands of magnitude 0.5–4.2 earthquakes were estimated using spectral amplitudes and first motion directions. Accurate relative locations were determined for several hundred earthquakes. The combined use of fault plane solutions and accurate relative locations provides a means for determining the orientation of active faults in the crust.

3 THE SEISMIC NETWORK AND DATA

The earthquakes reported here were recorded by the South Iceland Lowland (SIL) network (Stefánsson et al. 1993; Böðvarsson et al. 1996). The first eight stations of the SIL array were installed in 1990 to monitor seismicity in the South Iceland seismic zone. The network now consists of 34 seismic stations monitoring the seismic zones in Iceland. The study area extends from 63.9°N, 21.5°W to 64.2°N, 21.0°W. Two of the stations in or close to the study area were installed in October 1996. These are stations *kro* in Figure 1 and station *san* at 64.056°N, 21.570°W, just west of the area covered in Figure 1.

The digital, three component stations of the network are connected to a common data center via telephone lines. The data is sampled at 100 Hz, has 136 dB dynamic range and resolution better than 90 dB. The central processor automatically identifies and locates seismic events and estimates fault plane solutions and other source parameters. The automatic processing is extensively checked by the network staff. The station spacing in southern Iceland is 15–40 km. For the Hengill area the detection threshold of the system is close to $M_w = 0.0$ but here we consider only events with $M_w \geq 0.5$. These are usually located with 4–5 stations and the estimated location uncertainty is typically ± 1–1.5 km horizontally and ± 4 km vertically. After the addition of the new stations the location uncertainty is usually ± 1–1.5 km horizontally and

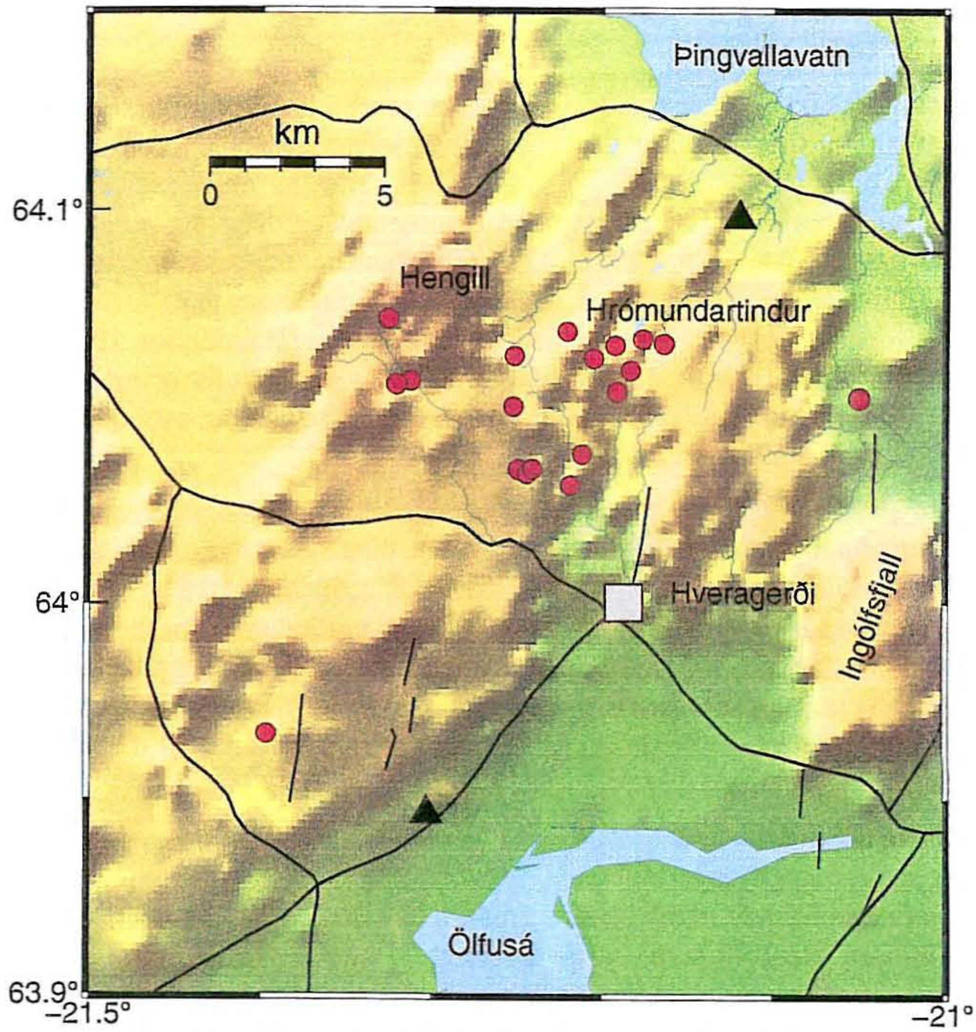

Figure 2. *The epicenters of earthquakes of magnitude $M_w = 3.5$ and larger in the Hengill area during 1993–1996 (red dots). The black triangles denote seismic stations.*

vertically.

4 SEISMICITY

The main activity in the present seismic swarm lies inside the 10 km wide rift zone. The swarm is composed of several minor clusters, elongated approximately E-W to ENE-WSW (Figure 1). Near the inferred location of the triple junction, close to station *bja* in Figure 1, there is a second clustering of earthquakes. The epicentral distribution in the southern group expresses a westward continuation of the SISZ, trending slightly south of the E-W trend of the SISZ. Activity in the southern group correlates in time with the Hengill activity.

The main activity is outside the Hengill fissure swarm. Since the beginning of the seismic episode there has been a general westward migration of the activity into the fissure swarm and it has extended to the west outside the zone. Superimposed on the general westward migration there has been an oscillatory movement of epicenters between the seismically active areas on the time scale of days. This implies a migration velocity of 5–10 km/day.

From 1993 to 1996, about 20 M = 3.5 or larger earthquakes occurred in the Hengill area. Six of these occurred during the August 1994 cluster and were located near the center of activity

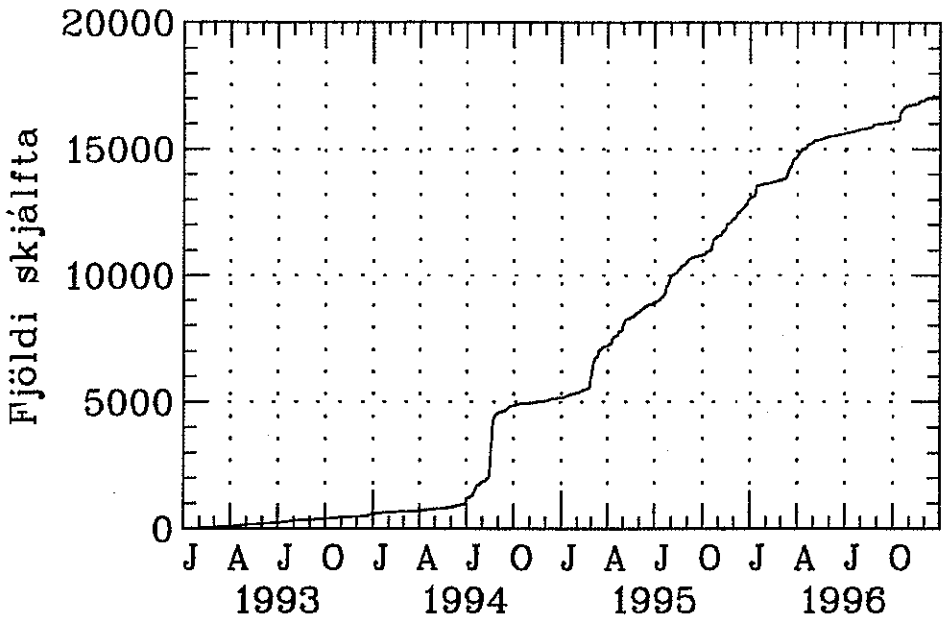

Figure 3. *Accumulated number of located earthquakes in the Hengill area from January 1993 to December 1996. The seismic episode began in July 1994. From April to December 1996 the activity was comparable to activity before the onset of the episode.*

(64.05°N, 21.2°W, Figures 1 and 2). The last big quake occurred in October 1996 north of Ingólfsfjall, near the eastern border of the study area.

From January 1993 to July 1994, the number of recorded $M_w \geq 0.5$ events in the area was approximately 13 per week. The present activity started with numerous small (M = 0–2) earthquakes near Mt. Hrómundartindur in July 1994 (Figure 1). The seismic activity peaked in mid-August 1994 with almost 5000 events recorded during one week. This first phase culminated in four magnitude 4 earthquakes on N-S or E-W striking faults a few kilometers southwest of Mt. Hrómundartindur. After that the seismicity rate returned to "normal" (i.e. pre-July) values. A second burst of activity occurred in March 1995 after which the earthquake rate stayed fairly constant at about 150 events per week until April 1996, i.e. more than ten times higher than prior to July 1994 (Figure 3). The last burst of activity during the study period was in October 1996 with one magnitude 4.2 earthquake and several hundred smaller events. Apart from that the seismicity rate has been comparable to pre-episode values since April 1996.

5 FOCAL MECHANISMS

Fault plane solutions for all located earthquakes are obtained by systematically searching over the entire parameter space for strike, dip and rake and comparing predicted polarities and spectral amplitudes to observations (Slunga 1981; Rögnvaldsson and Slunga 1993). The orientation of the P and T axis can be used to calculate the horizontal normal-force dipole size, S_h, on any vertical plane. S_h is given by

$$S_h = (\vec{N} \cdot \vec{T})^2 - (\vec{N} \cdot \vec{P})^2$$

where $\vec{N}$ is the unit normal of the given vertical plane and $\vec{T}$ and $\vec{P}$ are unit vectors parallel to the T and P axis respectively. S_h will be in the range -1 to 1 with $-1 \leq S_{h,min} \leq 0$ and $0 \leq S_{h,max} \leq 1$. Any fault plane solution can be displayed as a "stress square" plot, i.e. by plotting $S_{h,max}$ against $|S_{h,min}|$ (Slunga 1991; Rögnvaldsson and Slunga 1994). Fault plane

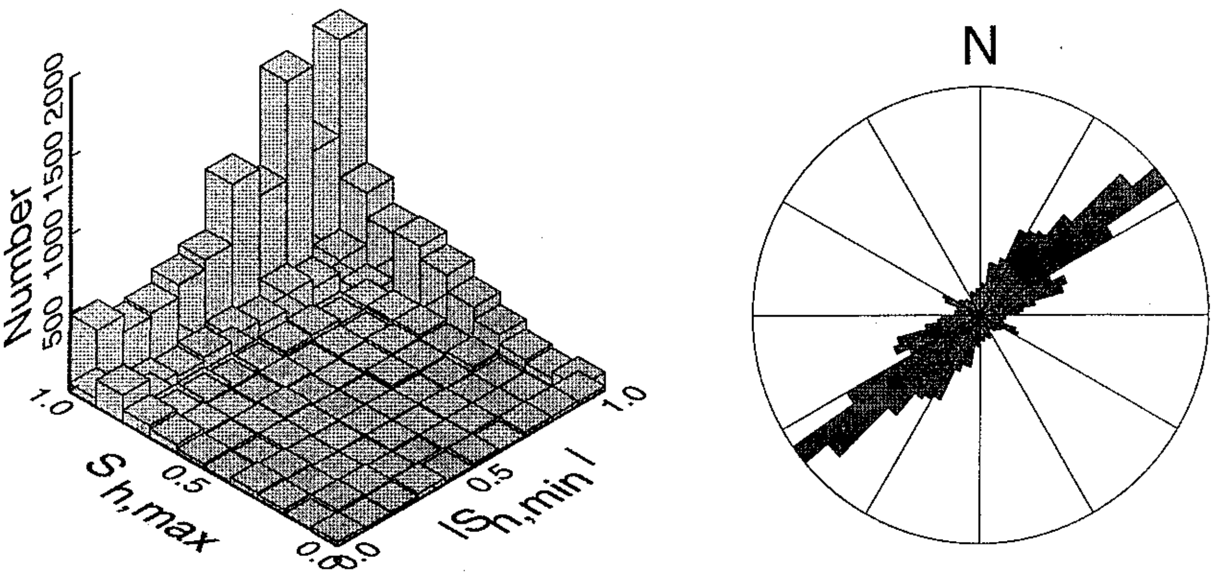

Figure 4. *Type of faulting in more than 10000* $0.5 \leq M_w \leq 3.9$ *earthquakes in the Hengill area (left). Strike slip on a vertical plane will have* $|S_{h,min}| = S_{h,max} = 1$*, dip slip on a vertical plane has* $|S_{h,min}| = S_{h,max} = 0$ *while for dip slip on a plane dipping 45° (normal faulting)* $|S_{h,min}| = 0$*,* $S_{h,max} = 1$ *and for reverse faulting* $|S_{h,min}| = 1, S_{h,max} = 0$*. Most of the earthquakes are strike-slip events but normal faulting events are also common. The rose diagram shows the direction of maximum horizontal compression released in the earthquakes. The average direction is 53°E.*

solutions have been estimated for more than 10000 earthquakes from 1993 to 1996. To display mechanisms of thousands of earthquakes we divide the "stress square" into 0.1 by 0.1 bins and generate a histogram showing the number of events having optimal fault plane solutions with $|S_{h,min}|$ and $S_{h,max}$ within each bin (Figure 4). The most common mechanism observed for events in the Hengill area is strike-slip (i.e. $|S_{h,min}| = S_{h,max} = 1$) on sub-vertical N-S or E-W faults but normal faulting is also common. The rose diagram in Figure 4 shows the direction of maximum horizontal compression released in earthquakes in the Hengill area. The data are very consistent with a mean direction of 53°E.

The fault plane solutions of the largest events (M = 4.0–4.2) all suggest right lateral strike-slip movement on N-S or left-lateral slip on E-W striking faults. This is the same style of faulting as inferred for historical magnitude 7 earthquakes in the SISZ (Einarsson and Eiríksson 1982). The M = 4.1 October 1996 event is located just north of N-S trending fault that presumably has ruptured in a major earthquake. The stresses released in the present swarm are therefore significantly different from the stresses which have caused the main rifting episodes in the WRZ, judging from historical and geological evidence, but similar to the stresses released in recent earthquakes in the SISZ (Stefánsson et al. 1993). During rifting episodes the NW horizontal compression is the smallest and vertical compression the largest component of stress, giving rise to NE-SW oriented normal faulting. In the present swarm activity the minimum and maximum stress components are horizontal, causing strike-slip faulting.

From a temporary network operated in the Hengill area in 1981, Foulger (1988b) estimated focal mechanisms of 178 earthquakes. Half of these data required a component of volume change to fit the polarity data and were interpreted as thermal cracking events due to cooling of rock at depth. Only eight of the 178 events were larger than M = 0.5 and of these two required a non-double-couple focal mechanism. The shear events exhibited faulting ranging from strike-slip on subvertical N-S or E-W planes, to normal faulting on NE oriented planes.

Since the SIL network is not dense enough to warrant complex source modelling of microearthquakes in the Hengill area, we seek only the simplest model that can explain the data, i.e. shear faulting without any volume component. As seen in Figure 4, our results obtained assuming only double-couple sources are very consistent. Data recorded after two close stations were added to the network give similar results as obtained with the sparser network recording most of the data in Figure 4. This and previous testing of the fault plane solution algorithm (Slunga 1980, 1981, 1982; Rögnvaldsson 1992; Rögnvaldsson and Slunga 1993) argues against systematic errors giving rise to the observed consistency. While our data can not exclude non-double-couple sources we suggest that even if present in our dataset, such events do not change the main results.

6 ACCURATE RELATIVE LOCATIONS

When several earthquakes occur in tight clusters, the arrival time differences between events can be determined with great accuracy through cross-correlation of their waveforms. The precise arrival time differences can give extremely accurate relative locations for a group of similar earthquakes. The arrival time differences are used not only for determining the relative locations of events within a cluster but also to constrain the absolute location of each event. The arrival time differences are much less sensitive to inaccuracies in the velocity model than are absolute arrival times. Therefore absolute locations constrained also by arrival time differences will be less affected by errors in the velocity model than if only absolute timing is used. The main source of error in our location procedure is uncertainties in the velocity gradient at the source, rather than uncertainties in structure between source and receiver (Slunga et al. 1995).

After relocation, the earthquakes in a cluster often appear to be distributed along a single plane. How well their distribution fits a plane is readily estimated by determining the best fitting plane through the hypocenters. An obvious interpretation of a plane through a cluster of microearthquakes is that the plane represents a single fault on which the earthquakes occurred. The fault plane solutions of individual earthquakes should then agree with the orientation of the plane determined from locations. Other possible explanations of why several earthquakes would line up along a plane include a common triggering mechanism (e.g. hydrofracturing) or an existing zone of weakness and, of course, coincidence. In none of these cases would one expect the fault planes of individual earthquakes to be parallel with the best fitting plane through the hypocenters.

The relative location uncertainties are typically 5–50 m. The mean distance of events from the best fitting plane should therefore not be more than a few tens of meters, if this plane is the common fault plane of the earthquakes. We have chosen a threshold value of 50 m, i.e. if the mean distance of earthquakes from the best fitting plane is greater we do not interpret the plane as a fault plane for the cluster. For very dense clusters (a few hundred meters across), the orientation of the best fitting plane may be poorly constrained, even if the average distance of events from the plane is small.

The combined use of accurate relative locations and fault plane solutions has been utilized to map fault planes within the SISZ (Slunga et al. 1995; Rögnvaldsson and Slunga 1994). The relative location procedure described by Slunga et al. (1995) was used to relocate more than

1600 earthquakes in the Hengill area, composing about 40 clusters. Each cluster comprises 10–200 earthquakes. For 28 of these groups we have found that the relocated earthquakes can be used to estimate the orientation of a common fault plane for the group. Two examples are shown in Figure 5. The upper pair shows a cluster of 22 events (location A in Figure 6) that

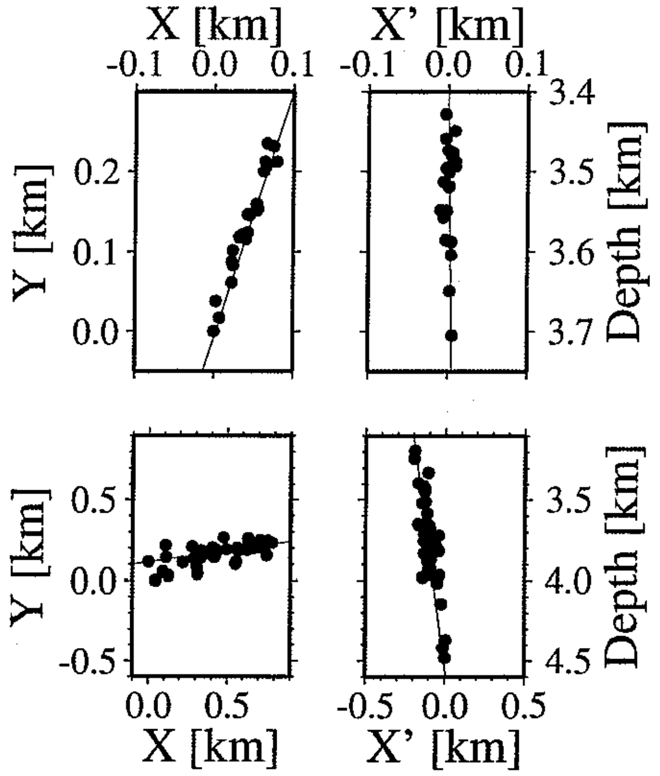

Figure 5. *Relative location of earthquakes in two earthquake clusters. The left column is a mapview of epicenters, in the right column a depth section. The Y-axis is north, X is east and the X'-axis is at right angles to the strike direction of the best fitting plane through the hypocenters. The cluster in the top row is located at A in Figure 6, the cluster in the bottom row at B.*

define a vertical plane striking 18°E. The lower pair is a cluster of 45 earthquakes located at B in Figure 6, delineating a plane striking 82°E and dipping 83° to the south. The mean distance of hypocenters from the best fitting plane is 5 m and 27 m, respectively, for the two clusters. Fault plane solutions show right-lateral strike-slip on northerly striking, near-vertical planes for events in cluster A. Faulting in cluster B is left-lateral strike-slip on steeply dipping E-W striking planes. The distinction between fault plane and auxiliary plane is done on bases of the relative locations.

Most of the earthquakes occur at depths of 2–6 km. Figure 6 shows the projection of the estimated fault planes up to the surface. Faults near the transform zone have northerly strikes, in agreement with field observations. Within the Hengill area the fault strikes are more varied, with N-S, E-W and N25°E being the most common directions. The N-S and E-W orientations are compatible with the present stress field while earthquakes on N25°E planes are probably on older reactivated faults.

The depth determination for earthquakes in the Hengill area, recorded before the installation of stations *kro* and *san*, was poor due to the unfavourable station distribution. Estimated uncer-

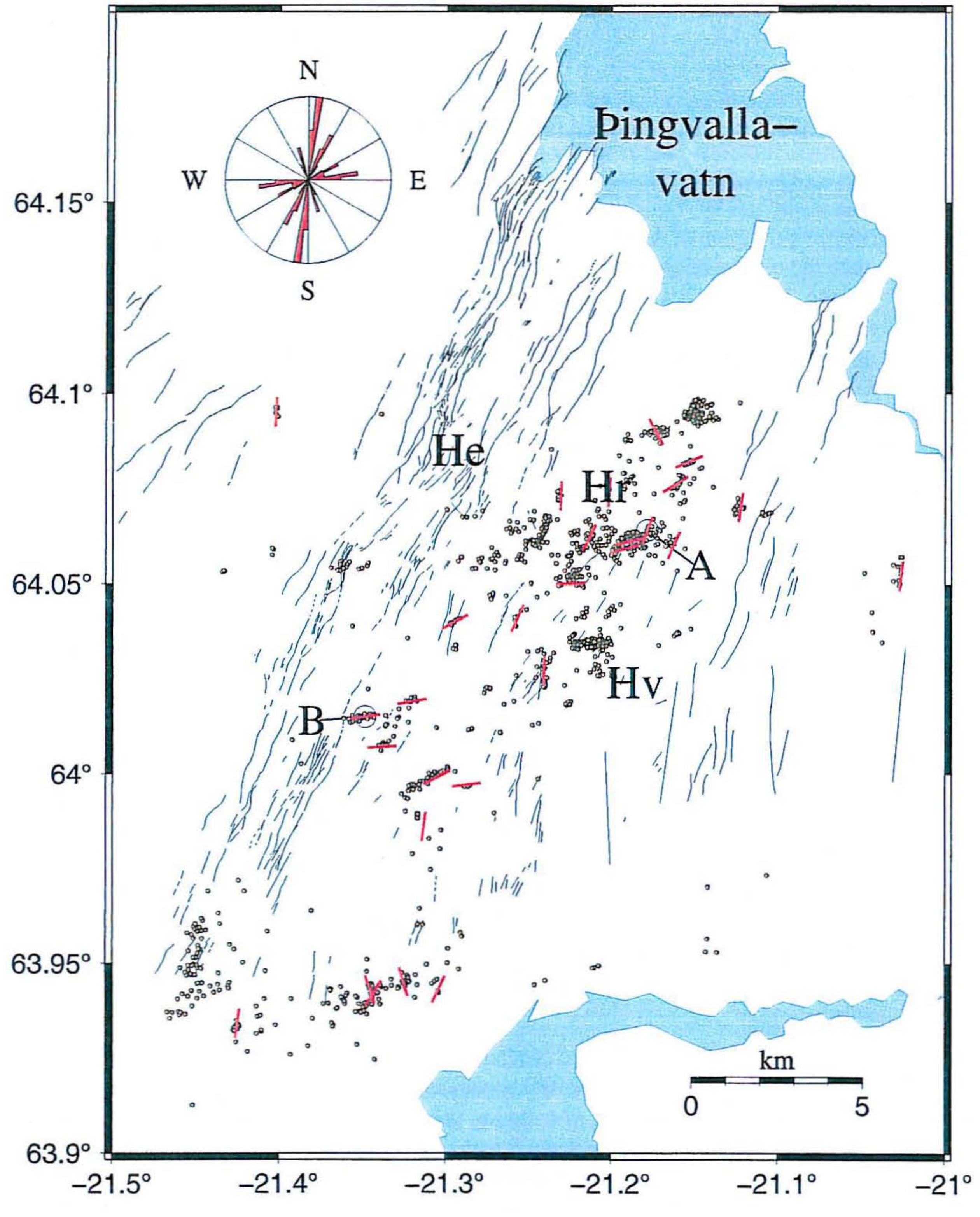

Figure 6. *The red lines show the location and orientation of fault planes estimated from the relative location of earthquakes. The black lines are mapped surface faults (Sæmundsson 1995). The inset rose diagram shows the orientation of the 28 faults mapped using accurate relative locations of earthquakes. A and B denote the locations of the earthquake clusters shown in Figure 5.*

tainty was typically ±4 km and often more. After addition of the two stations the estimated uncertainty in hypocentral depth is ±1–1.5 km. For the 1680 relocated earthquakes the estimated depth uncertainty is usually less than ±1 km. Thus the combined joint hypocentral determination and relative location procedure provides more accurate depth estimates than conventional single-event location procedures applied to data with far better station coverage.

7 DISCUSSION AND CONCLUSIONS

In general the long duration of the Hengill earthquake sequence suggests continued source activity, rather than the release of accumulated stress. Ongoing stable, ductile motion at depth might be such a source. If the activity was a gradual release of stress the swarm would probably have ended after the large earthquakes in the initial phase. However, the earthquakes resumed farther west. An alternative explanation of the prolonged activity would be dilatation of the region as a whole in the presence of high fluid pressure. It has been suggested that magma pressure below Mt. Hrómundartindur has increased, causing the observed seismicity and dilatation (Björnsson and Rögnvaldsson 1995; Sigmundsson et al. 1997).

The fault plane solutions of more than 10000 microearthquakes show that strike-slip is the dominant type of faulting in the 1994–96 seismic episode in the Hengill area. This part of the divergent plate boundary therefore appears to be in a mode of strain release compliant with the general E-W transform motion in the Reykjanes peninsula and the SISZ. In the present mode the maximum horizontal compression (oriented NE) is larger than the vertical stress component. This mode has probably been prevailing since a large normal faulting episode took place in the WRZ in 1789. Historical records show that farmhouses in the vicinity of station *bja* (Figure 1) repeatedly collapsed in earthquakes during the 18th century and earlier but never after the 1789 rifting event (Halldórsson 1996). The 1789 episode increased horizontal compression in and on both sides of the Hengill fissure swarm and subsequently changed the type of faulting from normal faulting to strike-slip. Such a change in the mode of strain release with time has earlier been proposed for the SISZ (Stefánsson and Halldórsson 1988) and the Reykjanes peninsula (Einarsson 1991).

A 25–30 km long section of the plate boundary west of the present seismic swarm is seismically quiet and, according to the historical seismic record, has been so since 1789. The locked section may eventually rupture in a relatively large (M = 6–7) earthquake. Such an event may suffice to change the mode of faulting at some locations from strike-slip dominated to predominantly normal faulting.

Accurate relative locations and improved absolute locations, based on relative timing, provide important information on a variety of crustal processes and conditions. The advantages of the method are especially evident in areas of complex velocity structure, e.g. near active volcanos. We have only applied this technique to a small part of the available data and have concentrated on estimating fault orientations. These results will provide additional constraints in the inversion of fault plane solutions to estimate the stress tensor in the area (Lund and Slunga 1998). Estimates of the stress tensor may in turn provide the means to monitor changes in the mode of strain release in the area.

Acknowledgements
This work was partly financed by the Icelandic Research Council, grant 95–N–701, and the European Commission Environment and Climate Programme, contract ENV4-CT96-0252.

8 REFERENCES

Árnason, K. 1993. Jarðhiti á Ölkelduhálssvæði (geothermal activity near Ölkelduháls). *Skýrsla Orkustofnunar* OS–93037/JHD–10. Orkustofnun, Reykjavík. In Icelandic with English summary.

Árnason, K., G.I. Haraldsson, G.V. Johnsen, G. Þorbergsson, G.P. Hersir, K. Sæmundsson, L.S. Georgsson and S.P. Snorrason 1985. Nesjavellir. jarðfræði– og jarðeðlisfræðileg könnun 1985 (Nesjavellir, geological and geophysical prospecting 1985). *Skýrsla Orkustofnunar* OS–93037/JHD–10. Orkustofnun, Reykjavík. In Icelandic with English summary.

Björnsson, G. and S.Th. Rögnvaldsson 1995. Upptök jarðskjálfta á Hengilssvæði árin 1992–1994 (earthquake epicenters in the Hengill area 1992–1994). *Greinargerð Orkustofnunar* GrB/SThR–95/01. Orkustofnun, Reykjavík. In Icelandic.

Böðvarsson, R., S.Th. Rögnvaldsson, S.S. Jakobsdóttir, R. Slunga and R. Stefánsson 1996. The SIL data acquisition and monitoring system. *Seism. Res. Lett.* 67, 35–46.

Einarsson, P. 1991. Earthquakes and present–day tectonism in Iceland. *Tectonophysics* 189, 261–279.

Einarsson, P. and J. Eiríksson 1982. Earthquake fractures in the districts Land and Rangárvellir in the South Iceland seismic zone. *Jökull* 32, 113–120.

Foulger, G.R. 1988a. Hengill triple point, SW-Iceland: 1. Tectonic structure and the spatial and temporal distribution of local earthquakes. *J. Geophys. Res.* 93, 13493–13506.

Foulger, G.R. 1988b. Hengill triple point, SW Iceland: 2. Anomalous earthquake focal mechanisms and implications for process within the geothermal reservoir and at accretionary plate boundaries. *J. Geophys. Res.* 93, 13507–13523.

Halldórsson, P. 1996. Yfirlit um jarðskjálftasögu Íslands (catalogue of historical earthquakes in Iceland). Unpublished manuscript, in Icelandic.

Halldórsson, P. and R. Stefánsson 1986. *Jarðskjálftar á Hengilssvæði, áhrifamat fyrir Nesjavelli* (earthquakes in the Hengill area, intensity estimates for Nesjavellir). Report, Veðurstofa Íslands, Reykjavík. In Icelandic.

Hersir, G.P., G. Björnsson and A. Björnsson 1990. Eldstöðvar og jarðhiti á Hengilssvæði (volcanos and geothermal activity in the Hengill area). *Skýrsla Orkustofnunar* OS–90031/JHD–06. Orkustofnun, Reykjavík. In Icelandic with English summary.

Lund, B. and R. Slunga 1998. Stress tensor inversion using detailed microearthquake information and stability constraints: application to the South Iceland seismic zone. *J. Geophys. Res.*, submitted.

Rögnvaldsson, S.Th. 1992. *Fault plane solutions by combined use of polarities and body wave amplitudes.* Dissertation for licentiate degree, Uppsala University, Uppsala, Sweden.

Rögnvaldsson, S.Th. and R. Slunga 1993. Routine fault plane solutions for local and regional networks: a test with synthetic data. *Bull. Seism. Soc. Am.* 11, 1247–1250.

Rögnvaldsson, S.Th. and R. Slunga 1994. Single and joint fault plane solutions for microearthquakes in South Iceland. *Tectonophysics* 273, 73–86.

Rögnvaldsson, S.Th., G. Guðmundsson, K. Ágústsson, S. Jakobsdóttir and R. Stefánsson 1996. Recent seismicity near the Hengill triple-junction, SW-Iceland. In: B. Þorkelsson (editor), *Seismology in Europe.* Papers presented at the XXV ESC General Assembly, Reykjavík, Iceland, September 9–14, 1996. ISBN–9979–60–235–X, 461–466.

Rögnvaldsson, S.Th., K. Ágústsson, B.H. Bergsson and G. Björnsson 1998. Jarðskjálftamælanet í nágrenni Reykjavíkur - lýsing á mælaneti og fyrstu niðurstöður (seismic network near Reykjavík - network description and first results). *Rit Veðurstofu Íslands* VÍ–R98001–JA01. Veðurstofa Íslands, Reykjavík. In Icelandic.

Sigmundsson, F., P. Einarsson, S.Th. Rögnvaldsson, G. Foulger, K. Hodkinson and G. Þorbergsson 1997. 1994–1995 seismicity and deformation at the Hengill triple junction, Iceland: triggering of earthquakes by an inflating magma chamber in a zone of horizontal shear stress. *J. Geophys. Res.* 102, 15151–15161.

Slunga, R. 1980. International seismological datacenter: an algorithm for associating reported arrivals to a global network into groups defining seismic events. *Technical report* C 20386–T1. Swedish National Defence Research Establishment, Sweden.

Slunga, R. 1981. Earthquake source mechanism determination by use of body–wave amplitudes - an application to Swedish earthquakes. *Bull. Seism. Soc. Am.* 71, 25–35.

Slunga, R. 1982. Research on Swedish earthquakes 1980–1981. *Technical report* C 20477–T1. Swedish National Defence Research Establishment, Sweden.

Slunga, R. 1991. The Baltic shield earthquakes. *Tectonophysics* 189, 323–331.

Slunga, R., S.Th. Rögnvaldsson and R. Böðvarsson 1995. Absolute and relative location of similar events with application to microearthquakes in southern Iceland. *Geophys. J. Int.* 123, 409–419.

Sæmundsson, K. 1967. Vulkanismus und Tektonik des Hengill-Gebietes in SW-Island. *Acta Nat. Isl.*, 105 pp.

Sæmundsson, K. 1995. Hengill, geological map (bedrock) 1:50000.

Stefánsson, R. and P. Halldórsson 1988. Strain build-up and strain release in the South Iceland seismic zone. *Tectonophysics* 152, 267–276.

Stefánsson, R., R. Böðvarsson, R. Slunga, P. Einarsson, S. Jakobsdóttir, H. Bungum, S. Gregersen, J. Havskov, J. Hjelme and H. Korhonen 1993. Earthquake prediction research in the South Iceland seismic zone and the SIL project. *Bull. Seism. Soc. Am.* 83, 696–716.

Toomey, D.H. and G.R. Foulger 1989. Tomographic inversion of local earthquake data from the Hengill–Grensdalur central volcano complex, Iceland. *J. Geophys. Res.* 94, 17497–17510.

Tryggvason, E. 1990. Höggun Almannagjár (displacements on the Almannagjá fault). *Skýrsla Norrænu eldfjallastöðvarinnar* 9001. Norræna eldfjallastöðin, Reykjavík. In Icelandic.

ISSN 1025-0565
ISBN 9979-878-13-4

Kápumynd: Klósigar (vatnsklær)
Ljósm.: Guðmundur Hafsteinsson, veðurfræðingur